Journal of Materials Chemistry

Cite this: J. Mater. Chem., 2011, 21, 7248

www.rsc.org/materials

PAPER

Molecular engineering of push-pull chromophore for efficient bulk-heterojunction morphology in solution processed small molecule organic photovoltaics†

Haye Min Ko,[a] Hyunbong Choi,[a] Sanghyun Paek,[a] Kyungjun Kim,[a] Kihyung Song,[b] Jae Kwan Lee[c] and Jaejung Ko*[a]

Received 15th February 2011, Accepted 17th March 2011
DOI: 10.1039/c1jm10667h

The synthesis and characterization of new push-pull chromophores, bisDMFA-diTh-CA, bisDMFA-diTh-MMN, and bisDMFA-diTh-MIMN from 5′-(4-(bis(9,9-dimethyl-9*H*-fluoren-2-yl)aniline (bisDMFA) electron donating, dithiophene bridging, and various electron withdrawing moieties, cyanoacrylic acid (CA), methylene malononitrile (MMN), and methylene indenylidene malononitrile (MIMN), were demonstrated for efficient solution processed BHJ solar cells. The photophysical properties, the hole mobilities from the space charge limitation of current (SCLC) *J-V* characteristics, and surface morphologies of these materials/PCBM bulk-heterojunction films were also investigated. The best power conversion efficiency of 3.66% (±0.12) with J_{sc} = 11.82 mA/cm^2, FF = 0.35, and V_{oc} = 0.90 V was observed in the BHJ film fabricated with the bisDMFA-diTh-MMN/C_{71}-PCBM composite with 3% 1-chloronaphthalene (CN), which is an efficiency ~82% and ~49% higher than before and after post-annealing without treatment of CN, respectively.

Introduction

Solution processed organic solar cells based on bulk-heterojunction (BHJ)[1,2] materials comprising small molecule chromophores and fullerene derivatives have offered special opportunities showing their promising power-conversion efficiencies (PCE) of above 4% as attractive alternatives to π-conjugated (semiconducting) polymers.[3,4] Although the BHJ devices fabricated by small molecule chromophore present lower efficiency than ~7% that by polymers,[5,6] these approaches by small molecules seem to fascinate more than the polymer ones from the viewpoint of mass production for commercial application due to their low reproducibility for characteristics such as average molecular weight (M_w) and polydispersity index (PDI) as well as difficulty in purification.

Recently, materials based on a diketopyrrolopyrrole (DPP) core have been demonstrated, showing a comparable PCE of above 4% to polymer BHJ solar cells.[3,7,8] Since the DPP core unit has a uniquely planar conjugated bicyclic structure and electron-withdrawing properties,[9,10] its derivatives comprising a thiophene moiety can strongly induce intermolecular π–π interactions and a band-shift of longer wavelength absorption by intramolecular charge transfer from the thiophene chain to the DPP core.[3,7–9] And DPP-thiophene based small molecule donors have exhibited good phase-separating networks with fullerene derivative acceptors.

On the other hand, we have also focused on the development of new chromophores for small molecule BHJ solar cells, which are motivated by organic dyes in dye-sensitized solar cells (DSSC)[11,12] and push-pull chromophores in nonlinear optics (NLO) due to a strong structural similarity with small molecule chromophores reported in BHJ solar cells.[13–21] In this work, we have attempted the fabrication of a BHJ device comprising a fullerene acceptor and a 2-cyanoacrylic acid-4-(bisdimethylfluoreneaniline)dithiophene (**bisDMFA-diTh-CA**) donor,[22,23] which is well-known as JK-2 organic dye in DSSC dye and provides good performance and stability for dye-sensitized solar cells.[24,25] And we have synthesized the new push-pull chromophores, 2-((5′-(4-(bis(9,9-dimethyl-9*H*-fluoren-2-yl)amino)phenyl)-2,2′-bithiophen-5-yl) methylene)malononitrile (**bisDMFA-diTh-MMN**) and 2-(2-((5′-(4-(bis(9,9-dimethyl-9*H*-fluoren-2-yl)amino)phenyl)-2,2′-bithiophen-5-yl)methylene)-3-oxo-2,3-dihydro-1*H*-inden-1-ylidene) malononitrile (**bisDMFA-diTh-MIMN**), which have a more electron withdrawing moiety, similarly to the structure of **bisDMFA-diTh-CA**.

Herein, we report the synthesis and characteristics of the above push-pull chromophores (**bisDMFA-diTh-CA**, **bisDMFA-diTh-MMN**, and **bisDMFA-diTh-MIMN**)/PCBM BHJ films and their

[a]*Department of Advanced Material Chemistry, Korea University, Chungnam, 330-700, Korea. E-mail: jko@korea.ac.kr; Fax: +82-41-860-5396; Tel: +82-41-860-1337*
[b]*Department of Chemistry, Korea National University of Education, Chungbuk, 363-791, Korea*
[c]*Department of Green Energy Engineering & Research Center for Convergence Technology, Hoseo University, Chungnam, 336-795, Korea*
† Electronic supplementary information (ESI) available: AFM pictures. See DOI: 10.1039/c1jm10667h

application in solution processed BHJ solar cell. We have also demonstrated the efficient morphology of these BHJ films and PCBM using a processing additive, resulting in a significantly increased efficiency of the device (Scheme 1).

Experimental

Materials

5′-(4-(bis(9,9-dimethyl-9*H*-fluoren-2-yl)amino)phenyl)-2,2′-bithophene-5-carbaldehyde[22,23] and 2-(3-oxo-2,3-dihydro-1*H*-inden-1-ylidene)malononitrile[26,27] were synthesized according to the procedures in the literature.

Instruments and measurements

^{1}H- and ^{13}C-NMR spectra were obtained on a Varian Mercury 300 spectrometer, a Varian/Oxford As-500 (500 MHz) spectrometer. Chemical shift values were recorded as parts per million relative to tetramethylsilane as an internal standard unless otherwise indicated, and coupling constants in Hertz. Optimized structures were calculated by TD-DFT using the B3LYP functional and the 3–21G* basis set. The highest occupied molecular orbital (HOMO) and the lowest unoccupied molecular orbital (LUMO) energies were determined using minimized singlet geometries to approximate the ground state. UV-vis data was measured with a Perkin-Elmer Lambda 2S UV-visible spectrometer. Photoluminescence spectra were recorded on a Perkin LS fluorescence Spectrometer. Cyclic voltammetry (CV) was performed using VersaSTAT 3 (Princeton Applied Research). Methylene chloride was used as the solvent and 0.1 M of tetrabutyl ammonium hexafluorophosphate was used as the supporting electrolyte. A platinum rod electrode coated with the donor compounds, a platinum wire and an $Ag/AgNO_3$ (0.10 M) electrode were used as the working electrode, as the counter electrode and as the reference electrode, respectively. The measurements were done using a scan rate of 100 mV/s and ferrocenium/ferrocene redox couple was used as an internal reference. AFM measurements were performed with a Digital Instruments NanoScope IV in the tapping mode.

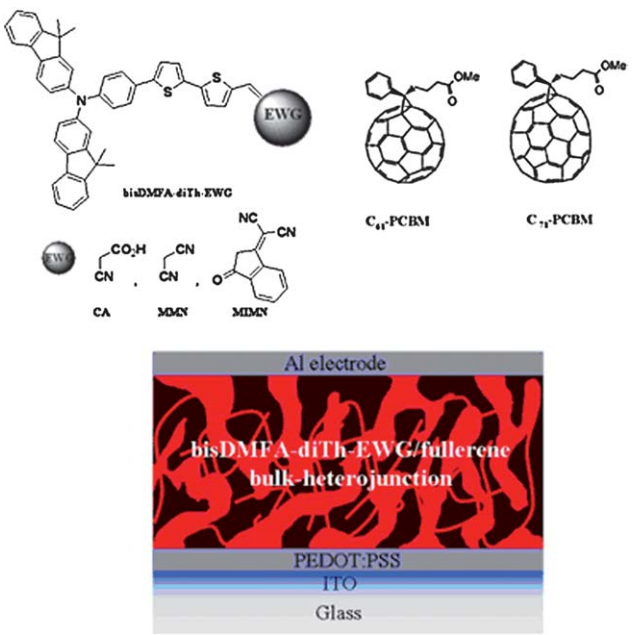

Scheme 1 Schematic depiction of the molecular structure of the new push-pull chromophores, **bisDMFA-diTh-CA**, **bisDMFA-diTh-MMN**, **bisDMFA-diTh-MIMN** and the structure of the solar cell device fabricated using these materials/fullerene BHJ active layer.

2-((5′-(4-(bis(9,9-dimethyl-9*H*-fluoren-2-yl)amino)phenyl)-2,2′-bithiophen-5-yl)methylene)malononitrile

Malononitrile (8.5 mg, 0.13 mmol) and piperidine (3∼5 drops) were added to a solution of 5′-(4-(bis(9,9-dimethyl-9*H*-fluoren-2-yl)amino)phenyl)-2,2′-bithophene-5-carbaldehyde (84 mg, 0.13 mmol) in CH_2Cl_2 (20 ml) at room temperature. The reaction mixture was heated under reflux for 12 h. Concentration and purification of the residue by flash column chromatography (Hex-EtOAc, 5 : 1) gave 2-((5′-(4-(bis(9,9-dimethyl-9*H*-fluoren-2-yl)amino)phenyl)-2,2′-bithiophen-5-yl)methylene)malononitrile (50 mg, 55%). Rf 0.5 (Hex-EtOAc, 5 : 1). ^{1}H-NMR (500 MHz, $CDCl_3$): δ 7.75 (s, 1H), 7.68–7.62 (m, 5H), 7.51 (d, 2H, $J = 8.5$ Hz), 7.43–7.39 (m, 3H), 7.35–7.24 (m, 8H), 7.20 (d, 2H, $J = 8.5$ Hz), 7.14 (dd, 2H, $J = 8.0$, 2.0 Hz), 1.43 (s, 12H) ^{13}C-NMR (75 MHz, $CDCl_3$): δ 155.4, 153.9, 150.1, 149.9, 148.7, 148.1, 146.8, 140.4, 138.9, 135.0, 133.2, 128.7, 127.2, 126.9, 124.2, 123.8, 123.6, 123.3, 122.7, 120.9, 119.7, 119.3, 115.6, 114.6, 113.7, 47.0, 27.2.

2-(2-((5′-(4-(bis(9,9-dimethyl-9*H*-fluoren-2-yl)amino)phenyl)-2,2′-bithiophen-5-yl)methylene)-3-oxo-2,3-dihydro-1*H*-inden-1-ylidene) malononitrile

2-(3-Oxo-2,3-dihydro-1*H*-inden-1-ylidene)malononitrile (23 mg, 0.11 mmol) was added to a solution of 5′-(4-(bis(9,9-dimethyl-9*H*-fluoren-2-yl)amino)phenyl)-2,2′-bithophene-5-carbaldehyde (76 mg, 0.11 mmol) in EtOH/THF (10 ml/6 ml) at room temperature. The reaction mixture was stirred for 12 h. The precipitate was filtered and washed repeatedly with ethanol to remove any remaining reactants. The product (90 mg, 94%) was recrystallized from ethanol. ^{1}H-NMR (500 MHz, DMSO-d_6): δ 8.67 (s, 1H), 8.50 (d, 1H, $J = 12.5$ Hz), 7.95–7.90 (m, 4H), 7.80–7.75 (m, 5H), 7.70–7.66 (m, 3H), 7.54 (dd, 3H, $J = 21.0$, 9.0 Hz), 7.35–7.28 (m, 6H), 7.11–7.07 (m, 4H), 1.38 (s, 12H) ^{13}C-NMR (125 MHz, DMSO-d_6): δ 187.5, 160.0, 154.9, 153.2, 152.2, 147.8, 146.9, 146.8, 146.2, 139.3, 138.2, 136.2, 135.5, 134.9, 134.7, 134.4, 133.4, 129.5, 127.1, 126.8, 126.6, 126.2, 125.3, 124.4, 123.5, 122.7, 122.5, 121.7, 121.2, 119.7, 119.0, 114.8, 114.6, 68.6, 46.5, 26.7.

Fabrication and characterization of solar cell devices

The BHJ films were prepared under optimized conditions according to the following procedure reported previously:[29] The indium tin oxide (ITO)-coated glass substrate was first cleaned with detergent, ultrasonicated in acetone and isopropyl alcohol, and subsequently dried overnight in an oven. Poly(3,4-ethylenedioxythiophene) : poly(styrenesulfonate) (PEDOT : PSS) in aqueous solution was spun-cast to form a film with a thickness of approximately 40 nm. The substrate was dried for 10 min at 140 °C in air, then transferred into a glove-box to spin-cast the photoactive layer. The donor/PCBM BHJ blend solutions (weight ratio, 1 : 2 or 1 : 3) were prepared in chlorobenzene at

a concentration of 30 mg/mL, and then spun-cast on top of the PEDOT layer. Then, the device was pumped down to lower than 10^{-7} torr and a ~100 nm thick Al electrode was deposited on top.

The solar cell's efficiencies were characterized under simulated 100 mW/cm^2 AM 1.5G irradiation from a 1000 W Xe arc lamp (Oriel 91193). The light intensity was adjusted with a Si solar cell that was double-checked with an NREL-calibrated Si solar cell (PV Measurement Inc.). The applied potential and measured cell current were measured using a Keithley model 2400 digital source meter. The current–voltage characteristics of the cell under these conditions were determined by biasing the cell externally and measuring the generated photocurrent. This process was fully automated using Wavemetrics software. The incident photon-to-current conversion efficiency (IPCE) spectra for the cells were measured on an IPCE measuring system (PV measurements).

Results and discussion

The synthetic procedures of **bisDMFA-diTh-CA**, **bisDMFA-diTh-MMN**, and **bisDMFA-diTh-MIMN** are shown in Scheme 2. **BisDMFA-diTh-CA**, 5′-(4-(bis(9,9-dimethyl-9*H*-fluoren-2-yl) amino)phenyl)-2,2′-bithophene-5-carbaldehyde[22,23] (**1**) and 2-(3-oxo-2,3-dihydro-1*H*-inden-1-ylidene)malononitrile[26,27] (**2**) were prepared according to a procedure reported previously. **BisDMFA-diTh-MMN** and **bisDMFA-diTh-MIMN** were synthesized by Knoevenagel condensation reaction using 5′-(4-(bis(9,9-dimethyl-9*H*-fluoren-2-yl)amino)phenyl)-2,2′ -bithophene-5-carbaldehyde (**1**) and an electron withdrawing group such as malononitrile, 2-(3-oxo-2,3-dihydro-1*H*-inden-1-ylidene) malononitrile (**2**).

Fig. 1 shows the UV-vis absorption spectra of the **bisDMFA-diTh-CA**, **bisDMFA-diTh-MMN**, and **bisDMFA-diTh-MIMN** in chlorobenzene solution and thin films. The corresponding optical properties are summarized in Table 1. As shown in Fig. 1, the absorption spectrum of **bisDMFA-diTh-CA**, **bisDMFA-diTh-MMN**, and **bisDMFA-diTh-MIMN** in solution shows

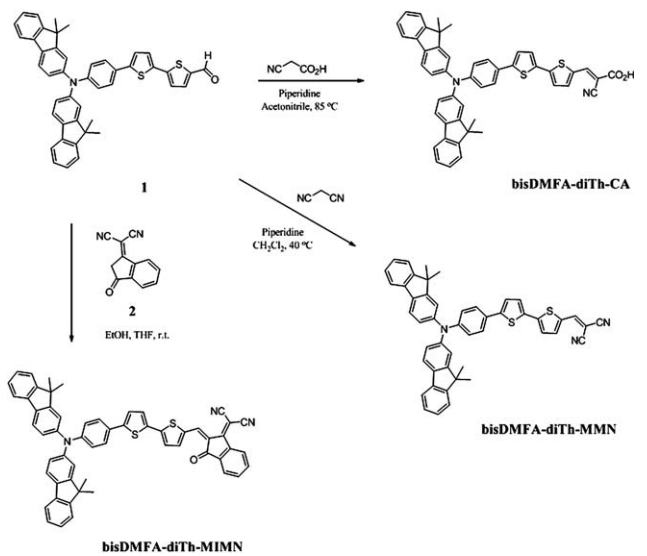

Scheme 2 Synthesis of the new push-pull chromophores, **bisDMFA-diTh-CA**, **bisDMFA-diTh-MMN**, **bisDMFA-diTh-MIMN**.

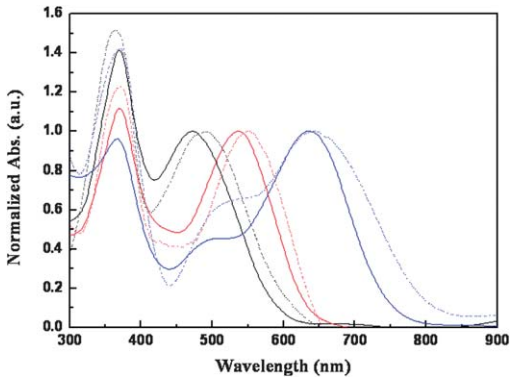

Fig. 1 Absorption spectra of **bisDMFA-diTh-CA** (black line), **bisDMFA-diTh-MMN** (red line) and **bisDMFA-diTh-MIMN** (blue line) in ClBz (solid line) and thin film (dot line).

intramolecular π–π* transition bands at 400~800 nm and a molar absorption coefficient of 20 791 M^{-1} cm^{-1} at 472 nm, 32 174 M^{-1} cm^{-1} at 536 nm, and 40 198 M^{-1} cm^{-1} at 636 nm, respectively. This indicates that the chromophore having the stronger electron withdrawing moiety exhibits a significantly red-shifted absorption spectrum and enhanced molar extinction coefficient due to its strong intramolecular charge transfer. In solid-state thin films, the absorption spectra of chromophores showed ~30 nm red-shift and broadened bands compared to those in solution.

Fig. 2 shows the cyclic voltammograms of **bisDMFA-diTh-CA**, **bisDMFA-diTh-MMN**, and **bisDMFA-diTh-MIMN** in methylene chloride solution. The corresponding electrochemical properties are also summarized in Table 1. The energy levels of the HOMO and LUMO of these materials were determined from these cyclic voltammetry (CV) spectra. A platinum rod electrode, a platinum wire and an Ag/AgNO$_3$ (0.10 M) electrode were used as the working electrode, as the counter electrode and as the reference electrode, respectively. The analyses were performed in an electrolyte consisting of a solution of 0.1 M tetrabutylammonium hexafluorophosphate (TBAPF$_6$) in methylene chloride at room temperature under nitrogen with a scan rate of 100 mV/s and ferrocenium/ferrocene redox couple was used as an internal reference. The HOMO and LUMO levels can be deduced from the oxidation and reduction onsets with the assumption that the energy level of ferrocene (Fc) is 4.8 eV below vacuum level. The CV of these materials in solid-state thin films could not be measured due to the stripping of the film on the electrode. Therefore, we determined the optical bandgap from calculations of the absorption thresholds from the absorption spectra of **bisDMFA-diTh** series in chlorobenzene. The HOMO level of the **bisDMFA-diTh-CA**, **bisDMFA-diTh-MMN**, and **bisDMFA-diTh-MIMN** determined in solution by CV are calculated as 4.883 eV, 4.916 eV, and 4.924 eV, respectively. From these results, we can roughly guess that the V_{oc} of the devices fabricated using these materials/PCBM BHJ active layers may be ~0.6 eV, respectively,[28] but the V_{oc} estimated in experiments was ~0.3 eV higher. These results will be discussed in more details below.

The performances of **bisDMFA-diTh-CA**, **bisDMFA-diTh-MMN**, and **bisDMFA-diTh-MIMN** were investigated through the application of photovoltaic devices fabricated with these

Table 1 Optical and redox parameters of the compounds

Compounds	λ_{abs}[a]/nm (ε/$M^{-1}cm^{-1}$)	λ_{PL}[a]/nm	$E_{onset,\ ox}$(V)/HOMO (eV)[b]	LUMO (eV)	E_{0-0} (eV)[c]
bisDMFA-diTh-CA	472 (20 791)	739, 745	0.083/−4.883	−2.803	2.08
bisDMFA-diTh-MMN	536 (32 174)	734	0.116/−4.916	−2.946	1.97
bisDMFA-diTh-MIMN	636 (40 198)	710	0.124/−4.924	−3.094	1.83

[a] Absorption spectra were measured in ClBz solution. [b] Redox potentials of the compounds were measured in CH_2Cl_2 with 0.1M $(n\text{-}C_4H_9)_4NPF_6$ with a scan rate of 100 mVs^{-1} (*vs.* Fc/Fc^+). [c] E_{0-0} was calculated from the absorption thresholds from absorption spectra of bisDMFA-diTh series in chlorobenzene.

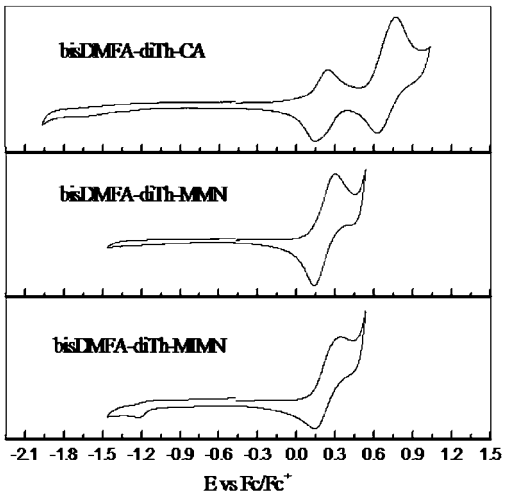

Fig. 2 Electrochemical characterization of **bisDMFA-diTh-EWG** series in dichloromethane/TBAHFP (0.1 M), scan speed 100 mV/s, potentials *vs.* Fc/Fc^+.

materials/$C_{61(or\ 71)}$-PCBM BHJ films. In the course of studying the characteristics of over 600 solar cells, the most efficient photovoltaic cells fabricated using **bisDMFA-diTh-CA** (or **bisDMFA-diTh-MMN**)/C_{71}-PCBM were optimized at a ratio of 1 : 2 approximately and **bisDMFA-diTh-MIMN**/C_{61}-PCBM was optimized at ratio of 1 : 3 approximately. These BHJ films were cast on top of a PEDOT : PSS layer by a spin speed of 1 500 rpm, and a 1.0 wt% of donor concentration in chlorobenzene. The optimum thickness of the **bisDMFA-diTh-CA**/C_{71}-PCBM, **bisDMFA-diTh-MMN**/C_{71}-PCBM, and **bisDMFA-diTh-MIMN**/C_{61}-PCBM BHJ films obtained under these conditions was approximately 80 nm, 73 nm, and 76 nm, respectively. The UV-visible absorption spectra of these BHJ films are shown in Fig. 3a.

The hole mobility was extracted the space charge limitation of current (SCLC) *J-V* characteristics obtained in the dark for hole-only ITO/PEDOT:PSS/Donor:PCBM/Au devices (Fig. 3b). The hole mobilities of **bisDMFA-diTh-CA**, **bisDMFA-diTh-MMN**, and **bisDMFA-diTh-MIMN** evaluated using the above Mott-Gurney Law ($\varepsilon = 3\varepsilon_0$) were 1.06×10^{-5} $cm^2/V{\cdot}s$, 4.86×10^{-5} $cm^2/V{\cdot}s$, and 3.57×10^{-5} $cm^2/V{\cdot}s$, respectively. The newly synthesized push-pull chromophores, **bisDMFA-diTh-MMN**, and **bisDMFA-diTh-MIMN** exhibited above 3.5 times higher mobility than **bisDMFA-diTh-CA**. These results note that the modification of the small molecular sensitizer by the carboxylic acid may negatively affect the transport properties of the hole carrier.

On the other hand, Fig. 4 shows the optimized structure of **bisDMFA-diTh-CA**, **bisDMFA-diTh-MMN**, and **bisDMFA-diTh-MIMN**, which were calculated by the time dependent-density functional theory (TD-DFT) using the B3LYP functional/3–21G* basis set. The orbital density of the HOMO of **bisDMFA-diTh-CA**, **bisDMFA-diTh-MMN**, and **bisDMFA-diTh-MIMN** are similarly observed on both **bisDMFA** and the dithiophene bridge. And the LUMO is located predominantly in the electron accepting core and dithiophene bridge, showing a general orbital distribution like push-pull chromophores. This calculation reveals that **bisDMFA** can partially play a role in stabilizing separated holes from excitons and improve the transport properties of the hole carrier.

Donor/PCBM BHJ films were prepared under optimized conditions according to the following procedure reported previously:[29] PEDOT : PSS (Baytron PH) was spun-cast on an

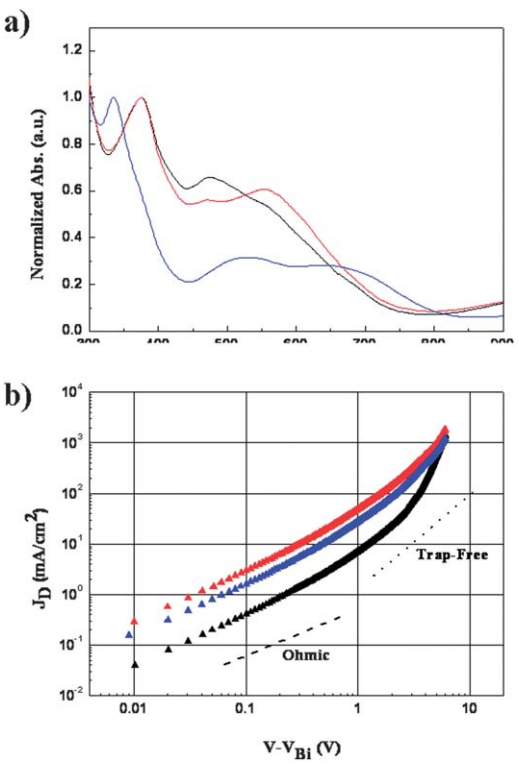

Fig. 3 (a) UV-Visible absorption spectra of **bisDMFA-diTh-CA**/C_{71}-PCBM films (black solid line), **bisDMFA-diTh-MMN**/C_{71}-PCBM films (red solid line), and **bisDMFA-diTh-MIMN**/C_{61}-PCBM films (blue line). (b) Hole-only devices (ITO/PEDOT:PSS/**bisDMFA-diTh-EWG**:PCBM/Au) with a thickness $L = 90 \pm 5$ nm.

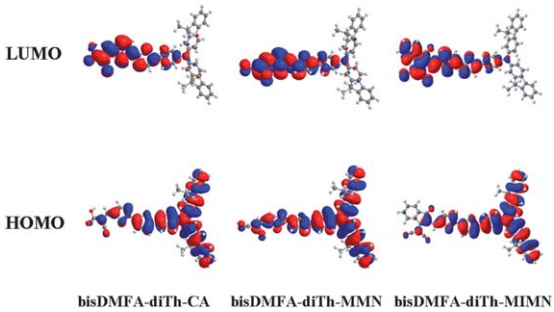

Fig. 4 Isodensity surface plots of **bisDMFA-diTh-CA**, **bisDMFA-diTh-MMN**, and **bisDMFA-diTh-MIMN**.

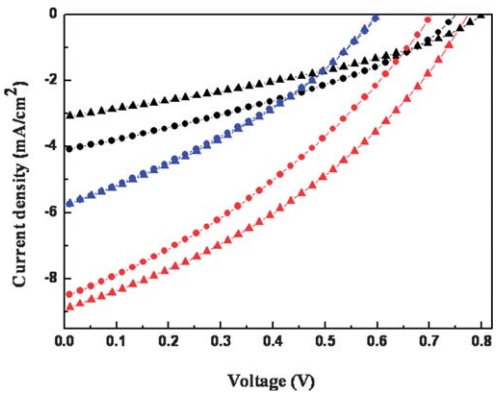

Fig. 5 Current (*J*)-voltage (*V*) curves under AM 1.5 conditions of device fabricated using **bisDMFA-diTh-CA**/C_{71}-PCBM BHJ active layer (black line), **bisDMFA-diTh-MMN**/C_{71}-PCBM films active layer (red line) and **bisDMFA-diTh-MIMN**/C_{61}-PCBM films (blue line) and annealed (triangle line).

indium tin oxide (ITO)-coated glass substrate from aqueous solution to form a film of a thickness around 40 nm. The substrate was dried for 10 min at 140 °C in air, then transferred into a glove-box to spin-cast the active layer. A solution containing the **bisDMFA-diTh-CA**/C_{71}-PCBM (or **bisDMFA-diTh-MMN**/C_{71}-PCBM, **bisDMFA-diTh-MIMN**/C_{61}-PCBM) in chlorobenzene was then spun-cast on top of the PEDOT : PSS layer. Subsequently, after the film was dried at room temperature, the device was pumped down in vacuum (< 10^{-6} torr; 1 torr ~ 133 Pa), and a ~100 nm thick Al electrode was deposited on top. The photovoltaic performances of the device were obtained under white light AM1.5G illumination from a calibrated solar simulator with an irradiation intensity of 100 mW/cm^2.

Fig. 5 shows the current (*J*)-voltage (*V*) curves under AM 1.5 conditions (100 mW per cm^2) of **bisDMFA-diTh-CA**/C_{71}-PCBM (or **bisDMFA-diTh-MMN**/C_{71}-PCBM, **bisDMFA-diTh-MIMN**/C_{61}-PCBM) BHJ solar cells with post-annealing at 100 °C, and the corresponding values are summarized in Table 2. As shown in Table 2, the devices fabricated with the **bisDMFA-diTh-MMN**/C_{71}-PCBM film exhibited two times better performances than with the **bisDMFA-diTh-CA**/C_{71}-PCBM and **bisDMFA-diTh-MIMN**/C_{61}-PCBM films. The most efficient devices have an PCE of 2.46% (±0.11), with a short-circuit current (J_{sc}) = 8.91 mA/cm^2, fill factor (*FF*) = 0.36, and open-circuit voltage (V_{oc}) = 0.77 V after post-annealing at 100 °C for 10 min, which is a ~22% higher efficiency than that before post-annealing. These results may be caused by the higher hole-mobility of **bisDMFA-diTh-MMN** and the morphology of the **bisDMFA-diTh-MMN**/C_{71}-PCBM film investigated by atomic force microscopy (AFM), resulting in the better phase-separated bicontinuous network with finer grains than those of the **bisDMFA-diTh-CA**/C_{71}-PCBM and **bisDMFA-diTh-MIMN**/C_{61}-PCBM films (see ESI).†

We have also attempted a more effective phase-separated morphology of BHJ composite using a processing additive, 1-chloronaphthalene (CN),[30,31] to provide an increased efficiency of the **bisDMFA-diTh-MMN**/C_{71}-PCBM BHJ device. Fig. 6a shows the current (*J*)-voltage (*V*) curves under AM 1.5 conditions (100 mW per cm^2) of the device with a BHJ film fabricated from the **bisDMFA-diTh-MMN**/C_{71}-PCBM composite with 3% CN. Indeed, the **bisDMFA-diTh-MMN**/C_{71}-PCBM BHJ device exhibited the significantly ~82% enhanced efficiency after addition of 3% CN in solution compared to that without additive, resulting in the best PCE of 3.66% (±0.13), with J_{sc} = 11.82 mA/cm^2, *FF* = 0.35, and V_{oc} = 0.90 V. Also this is ~49% higher than that after post-annealing in Table 2. This enhanced efficiency is mainly caused by the increase of J_{sc} and V_{oc}. The more phase-segregated morphology of the BHJ film fabricated with the **bisDMFA-diTh-MMN**/C_{71}-PCBM composite with 3% CN could increase the photocurrent of device (Fig. 6c). The incident-photon-to-current efficiency (IPCE) spectra as shown in Fig. 6b exhibit well-matched curves with their optical absorptions, resulting in the close correlation with their

Table 2 Photovoltaic performances of the BHJ polymer solar cells made of **bisDMFA-diTh-CA** or **bisDMFA-diTh-MMN**/C_{71}-PCBM (1 : 2) & **bisDMFA-diTh-MIMN**/C_{61}-PCBM (1 : 3)

Components[a]	J_{sc} (mA cm^{-2})	V_{oc} (V)	*FF* (%)	η (%)
bisDMFA-diTh-CA	4.11	0.749	34.78	1.07
bisDMFA-diTh-CA (annealed)	3.16	0.780	34.69	0.85
bisDMFA-diTh-MMN	8.54	0.705	33.35	2.01
bisDMFA-diTh-MMN (annealed)	8.91	0.774	35.74	2.46
bisDMFA-diTh-MIMN	5.64	0.628	32.08	1.14
bisDMFA-diTh-MIMN (annealed)	5.77	0.600	33.55	1.16

[a] The optimum devices were fabricated with **bisDMFA-diTh-CA** or **bisDMFA-diTh-MMN**/C_{71}-PCBM (1 : 2) & **bisDMFA-diTh-MIMN**/C_{61}-PCBM (1 : 3) films which were spin-cast at 1500 rpm from a chlorobenzene solution. The performances are determined under simulated 100 mW/cm^2 AM 1.5G illumination. The light intensity using calibrated standard silicon solar cells with a proactive window made from KG5 filter glass traced to the National Renewable Energy Laboratory (NREL). The active area of the device is 4 mm^2.

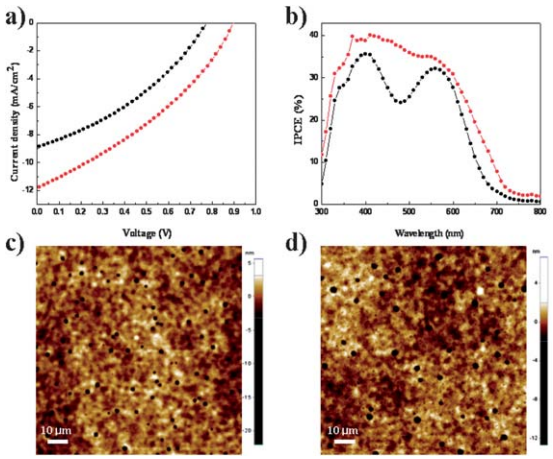

Fig. 6 (a) Current (*J*)-voltage (*V*) curves and (b) IPCE spectra under AM 1.5 conditions of device fabricated using **bisDMFA-diTh-MMN**/C_{71}-PCBM BHJ active layer with 3% CN (red line), and without 3% CN (black line). Tapping mode AFM surface topography of films cast from of **bisDMFA-diTh-MMN**/C_{71}-PCBM BHJ (c) without 3% CN (d) with 3% CN.

photocurrents in the *J*-*V* curves. Although V_{oc} is basically determined by the energy difference between the HOMO of the semiconducting polymer and the LUMO of the fullerene, we have observed from many experiments that changes in the morphology of the BHJ films can affect the V_{oc}. This might be caused by changes in the local internal field when the morphology of the BHJ material is changed. Beyond such speculation, we do not have a definitive explanation why the CN additive causes a large increase in V_{oc}.

Conclusions

In conclusion, we have demonstrated the synthesis and characterization of new push-pull chromophores, which comprise **bisDMFA** electron donating, dithiophene bridging, and various electron withdrawing moieties, for their application in solution processed BHJ solar cells. The chromophore having the stronger electron withdrawing moiety exhibits a significantly red-shifted absorption spectrum and enhanced molar extinction efficiency due to its strong intramolecular charge transfer in solution as well as in solid-state. A remarkable PCE of 3.66% (±0.12) was observed in the BHJ film fabricated with the **bisDMFA-diTh-MMN**/C_{71}-PCBM composite with 3% CN, showing ~82% and ~49% higher efficiencies compared to without treatment of CN and after post-annealing, respectively. These results obtained from the molecular engineering approaches shown in this study can give an important guide for developing new materials in solution-processed small molecule BHJ solar cells.

Acknowledgements

The research was supported by the WCU (the Ministry of Education and Science) program (Grant No. R 31-2008-0001- 10035-0), ITRC program (IITA 2008 C1090 0904 0013), and ERC (the Korean government [MEST]) program (No. R11-2009- 088-02001-0).

Notes and references

1 G. Dennler, M. C. Scharber and C. J. Brabec, *Adv. Mater.*, 2009, **21**, 1323.
2 A. C. Arias, J. D. Mackenzie, I. McCulloch, J. Rivnay and A. Salleo, *Chem. Rev.*, 2010, **110**, 3.
3 B. Walker, A. B. Tamayo, X. D. Dang, P. Zalar, J. H. Seo, A. Garcia, M. Tantiwiwat and T.-Q. Nguyen, *Adv. Funct. Mater.*, 2009, **19**, 3063.
4 B. Walker, C. Kim, T.-Q. Nguyen, *Chem. Mater. ASAP.*
5 H. Y. Chen, J. Hou, S. Zhang, Y. Liang, G. Yang, Y. Yang, L. Yu, Y. Wu and G. Li, *Nat. Photonics*, 2009, **3**, 649.
6 X. Zhan and D. Zhu, *Polym. Chem.*, 2010, **1**, 409.
7 A. B. Tamayo, B. Walker and T.-Q. Nguyen, *J. Phys. Chem. C*, 2008, **112**, 11545.
8 A. B. Tamayo, X. D. Dang, B. Walker, J. Seo, T. Kent and T.-Q. Nguyen, *Appl. Phys. Lett.*, 2009, **94**, 103301.
9 A. B. Tamayo, M. Tantiwiwat, B. Walker and T. Q. Nguyen, *J. Phys. Chem. C*, 2008, **112**, 15543.
10 L. Huo, J. Hou, H. Y. Chen, S. Zhang, Y. Jiang, T. L. Chen and Y. Yang, *Macromolecules*, 2009, **42**, 6564.
11 B. O'Regan and M. Gratzel, *Nature*, 1991, **353**, 737.
12 A. Hagfeldt, G. Boschloo, L. Sun, L. Kloo and H. Pettersson, *Chem. Rev.*, 2010, **110**, 6595.
13 P. V. Bedworth, Y. Cai, A. Jen and S. R. Marder, *J. Org. Chem.*, 1996, **61**, 2242.
14 N. Tirelli, S. Amabile, C. Cellai, A. Pucci, L. Regoli, G. Ruggeri and F. Ciardelli, *Macromolecules*, 2001, **34**, 2129.
15 P. F. Xia, X. J. Feng, J. Lu, S.-W. Tsang, R. Movileanu, Y. Tao and M. S. Wong, *Adv. Mater.*, 2008, **20**, 4810.
16 Y. J. Chang and T. J. Chow, *Tetrahedron*, 2009, **65**, 4726.
17 C. Herbivo, A. Comel, G. Kirsch, A. M. C. Fonseca, M. Belsley and M. M. M. Raposo, *Dyes Pigm.*, 2010, **86**, 217.
18 C. Sissa, V. Parthasarathy, D. Drouin-Kucma, M. H. V. Werts, M. Blanchard-Desce and F. Terenziani, *Phys. Chem. Chem. Phys.*, 2010, **12**, 11715.
19 F. Huang, K.-S. Chen, H.-L. Yip, S. K. Hau, O. Acton, Y. Zhang, J. Luo and A. K.-Y. Jen, *J. Am. Chem. Soc.*, 2009, **131**, 13886.
20 C. Duan, K.-S. Chen, F. Huang, H.-L. Yip, S. Liu, J. Zhang, A. K.-Y. Jen and Y. Cao, *Chem. Mater.*, 2010, **22**, 6444.
21 C. Duan, W. Cai, F. Huang, J. Zhang, M. Wang, T. Yang, C. Zhong, X. Gong and Y. Cao, *Macromolecules*, 2010, **43**, 5262.
22 S. Kim, J. K. Lee, S. O. Kang, J. Ko, J. H. Yum, S. Fantacci, F. D. Angelis, D. D. Censo, M. D. Nazeeruddin and M. Gratzel, *J. Am. Chem. Soc.*, 2006, **128**, 16701.
23 S. Kim, H. Choi, D. Kim, K. Song, S. O. Kang and J. Ko, *Tetrahedron*, 2007, **63**, 9206.
24 Y. Shirota, M. Kinoshita, T. Noda, K. Okumoto and T. Ohara, *J. Am. Chem. Soc.*, 2000, **122**, 11201.
25 H. Doi, M. Kinoshita, K. Okumoto and Y. Shirota, *Chem. Mater.*, 2003, **15**, 1080.
26 Y. Shang, Y. Wen, S. Li, S. Du, X. He, L. Cai, Y. Li, L. Yang, H. Gao and Y. Song, *J. Am. Chem. Soc.*, 2007, **129**, 11674.
27 Y. Cui, H. Ren, J. Yu, Z. Wang and G. Qian, *Dyes Pigm.*, 2009, **81**, 53.
28 M. C. Scharber, D. Mühlbacher, M. Koppe, P. Denk, C. Waldauf, A. J. Heeger and C. J. Brabec, *Adv. Mater.*, 2006, **18**, 789.
29 J. K. Lee, W. L. Ma, C. J. Brabec, J. Yuen, J. S. Moo, J. Y. Kim, K. Lee, G. C. Bazan and A. J. Heeger, *J. Am. Chem. Soc.*, 2008, **130**, 3619.
30 C. H. Woo, P. M. Beaujuge, T. W. Holcombe, O. P. Lee and J. M. J. Frechet, *J. Am. Chem. Soc.*, 2010, **132**, 15547.
31 C. V. Hoven, X.-D. Dang, R. C. Coffin, J. Peet, T.-Q. Nguyen and G. C. Bazan, *Adv. Mater.*, 2010, **22**, E63.